AD-A179 138 RECONSTRUCTION OF THE LEFT VENTRICLE FROM TWO ORTHOGONAL PROJECTION(U) PITTSBURGH UNIV PA CENTER FOR MULTIVARIATE ANALYSIS Z D BAI ET AL. OCT 86 TR-86-33 1/1

UNCLASSIFIED AFOSR-TR-87-0320 F49620-85-C-0008 F/G 6/5 NL

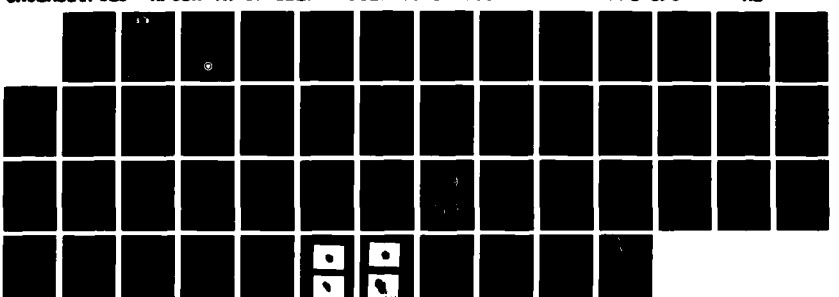

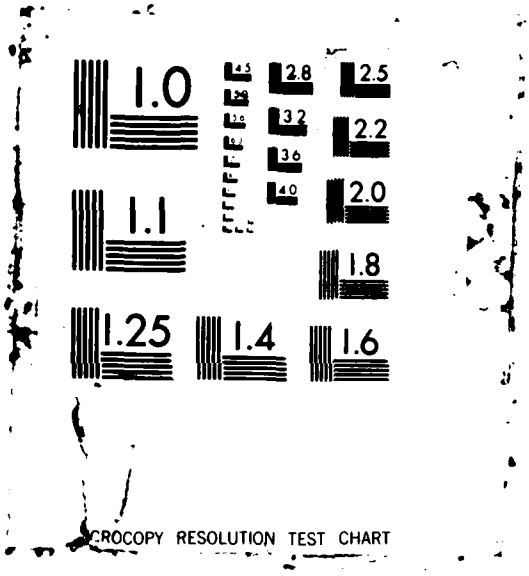
1.0
1.1
1.25
1.4
1.6
2.8
3.2
3.6
4.0
2.5
2.2
2.0
1.8
CROCOPY RESOLUTION TEST CHART

Unclassified
SECURITY CLASSIFICATION OF THIS PAGE

(2)

REPORT DOCUMENTATION PAGE

1a. REPORT SECURITY CLASSIFICATION: Unclassified	1b. RESTRICTIVE MARKINGS
2a. SECURITY CLASSIFICATION AUTHORITY	3. DISTRIBUTION/AVAILABILITY OF REPORT: Approved for public release; distribution unlimited
2b. DECLASSIFICATION/DOWNGRADING SCHEDULE	
4. PERFORMING ORGANIZATION REPORT NUMBER(S)	5. MONITORING ORGANIZATION REPORT NUMBER(S): AFOSR-TR- 87-0320
6a. NAME OF PERFORMING ORGANIZATION: University of Pittsburgh; 6b. OFFICE SYMBOL (If applicable)	7a. NAME OF MONITORING ORGANIZATION: AFOSR/NM
6c. ADDRESS (City, State and ZIP Code): Fifth Avenue Thackery Hall, Pittsburgh, PA 15260	7b. ADDRESS (City, State and ZIP Code): Bldg 410, Bolling AFB DC 20332-6448
8a. NAME OF FUNDING/SPONSORING ORGANIZATION: AFOSR; 8b. OFFICE SYMBOL (If applicable): NM	9. PROCUREMENT INSTRUMENT IDENTIFICATION NUMBER: F49620-85-C-0008
8c. ADDRESS (City, State and ZIP Code): Bldg. 410, Bolling AFB, DC 20332-6448	10. SOURCE OF FUNDING NOS.

PROGRAM ELEMENT NO.	PROJECT NO.	TASK NO.	WORK UNIT NO.
61102F	2304	A5	

11. TITLE (Include Security Classification): Reconstruction of the left ventricle from two orthogonal projection

12. PERSONAL AUTHOR(S): Professor P. R. Krishnaiah

13a. TYPE OF REPORT	13b. TIME COVERED	14. DATE OF REPORT (Yr., Mo., Day)	15. PAGE COUNT
Reprint	FROM _____ TO _____	October 1986	46

16. SUPPLEMENTARY NOTATION

17. COSATI CODES			18. SUBJECT TERMS (Continue on reverse if necessary and identify by block number)
FIELD	GROUP	SUB. GR.	

19. ABSTRACT (Continue on reverse if necessary and identify by block number)

ABSTRACT

A new method for reconstruction of the shape of the left ventricle from the biplane angiocardiograms is proposed. The approach utilizes a pair of orthogonal X-ray projection images. The shape of the ventricle is reconstructed by dividing these projection images into parallel slices and then being processed slice by slice sidewise. Each corresponding pair of slices form two one-dimensional projection profiles which are used to reconstruct a cross section of the ventricle.

Without using predefined models we proposed a new method to reconstruct the cross section under the assumption that the cross section is regular along the directions of projections and a monotonically nondecreasing or nonincreasing equal-divisor curve is available. A cross section is regular if it contains only one closed interval within the cross section along each ray of projection. The equal-divisor curve is defined within the cross section which divides each closed interval into two equal halves. Instead of solving the binary matrix directly we need only to obtain the equal-divisor curve, then the cross section is uniquely determined. We have proved that the cross section can be optimally reconstructed by minimizing an error index which is generated by the sum of the absolute difference between the original and estimated projection profiles. The algorithm has been tested on synthetic and X-ray pictures with better than 95% conformity for regular cross sections. The experiments show better results than any existing direct methods since it is based on a more flexible geometrical assumption. It also prevents the sensitive selection of mass model which dominates the results of model-based methods. Thus the algorithm is reliable and more generally fits real shapes of the ventricle.

20. DISTRIBUTION/AVAILABILITY OF ABSTRACT

UNCLASSIFIED/UNLIMITED ☐ SAME AS RPT ☐ DTIC USERS ☐

Unclassified

22a. NAME OF RESPONSIBLE INDIVIDUAL	22b. TELEPHONE (Include Area Code)	22c. OFFICE SYMBOL
Major Woodruff	(202) 767-5026	NM

DD FORM 1473, 83 APR — EDITION OF 1 JAN 73 IS OBSOLETE.

SECURITY CLASSIFICATION OF THIS PAGE

Center for Multivariate Analysis

University of Pittsburgh

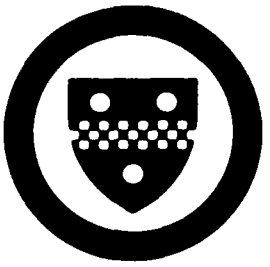

RECONSTRUCTION OF THE LEFT VENTRICLE FROM TWO ORTHOGONAL PROJECTIONS

By
Z. D. Bai, P. R. Krishnaiah, C. R. Rao, P. S. Reddy,
Y. N. Sun and L. C. Zhao
Center for Multivariate Analysis

October 1986
Technical Report 86-33

Center for Multivariate Analysis
Fifth Avenue, Thackeray Hall
University of Pittsburgh
Pittsburgh, PA 15260

*This work is partially supported by Siemens, Inc.

TABLE OF CONTENTS

ABSTRACT

A new method for reconstruction of the shape of the left ventricle from the biplane angiocardiograms is proposed. This approach utilizes a pair of orthogonal X-ray projection images. The shape of the ventricle is reconstructed by dividing these projection images into parallel slices and then being processed slice by slice stepwise. Each corresponding pair of slices form two one-dimensional projection profiles which are used to reconstruct a cross section of the ventricle.

Without using predefined models, we proposed a new method to reconstruct the cross section under the assumption that the cross section is regular along the directions of projections and a monotonically nondecreasing or nonincreasing equal-divisor curve is available. A cross section is regular if it contains only one closed interval within the cross section along each ray of projection. The equal-divisor curve is defined within the cross section which divides each closed interval into two equal halves. Instead of solving the binary matrix directly, we need only to obtain the equal-divisor curve, then the cross section is uniquely determined. We have proved that the cross section can be optimally reconstructed by minimizing an error index which is generated by the sum of the absolute difference between the original and estimated projection profiles. The algorithm has been tested on synthetic and X-ray pictures with better than 95% conformity for regular cross sections. The experiments show better results than any existing direct methods since it is based on a more flexible geometrical assumption. It also prevents the sensitive selection of mask model which dominates the results of model-based methods. Thus, the algorithm is reliable, and more generally fits real shapes of the ventricle.

CHAPTER 1

INTRODUCTION

In patients with cardiovascular diseases, left ventricular function is one of the major parameters to be considered in making therapeutic choices and determining prognosis. Left ventricular function is primarily evaluated by measurements of pressure and volume during a cardiac cycle. Although several indices based upon the volume measurements have been developed, accurate measurements of volume are not yet possible. Almost all methods of measurement are based upon an ellipse model. Even the biplane integration method based on Simpson's rule, the most accurate method of all, assumes an ellipsoid shape constructed around two axes for each cross section. Therefore, any method that can improve the accuracy of the measurement of cross sectional area is likely to improve accuracy of the method to measure the ventricular volumes. The present study was undertaken to investigate if the shape of each cross section can be predicted with better accuracy knowing the density of the dye (radiopaque dye injected to visualize the left ventricle) in two planes.

In this report we present a new method for reconstruction of the shape of the left ventricle from the biplane angiocardiograms. This approach utilizes a pair of orthogonal X-ray projection images for each ventricular phase in a cardiac cycle The projection image is a two-dimensional picture which is obtained by integrating the absorption function of the X-ray photons along the directions parallel to the optical axis of the camera sets. Obviously, the absorption function affected by the injected dye will influence the reconstructed results. For simplicity, we define the absorption coefficient of the dye to be unity to form a binary reconstruction problem just like all the other developed methods The shape of the ventricle is reconstructed by dividing these projections into slices and then being processed

slice by slice stepwise. Therefore, we reduce our three-dimensional problem into a two-dimensional problem by considering the object as a stack of parallel cross sections. Each cross section consists of one connected region and is reconstructed from its two one-dimensional projection profiles. Therefore, our problem can be stated as the reconstruction of a binary matrix from its row and column sums.

In Chapter 2 we describe our reconstruction problem and review some currently developed methods. In Chapter 3 some mathematical characteristics are explicated. Our algorithm and its implementation are discussed in Chapter 4. Some synthetic examples are also demonstrated. In Chapter 5, we describe an experiment by using two projection images from a bag of dye. The discussion of the experimental results and some suggestions for further improvements are given in Chapter 6.

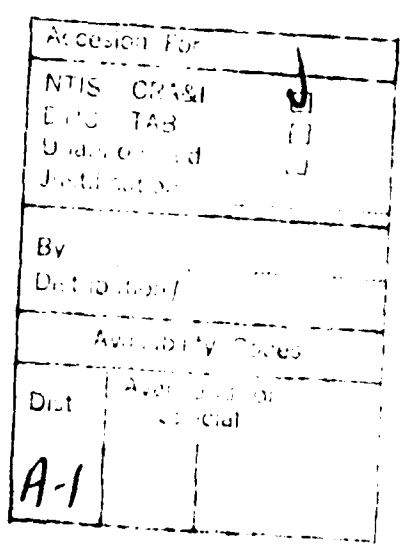

CHAPTER 2

PROBLEM DESCRIPTION AND LITERATURE REVIEW

The binary reconstruction problem may be stated as follows in terms of entries of a matrix X with m x n cells. Each cell is identified by the pair of numbers (i,j) and is represented by x_{ij}. x_{ij} may be 1 if the cell falls into the region of object or 0 otherwise. The problem is to estimate x_{ij} given the marginals

$$\sum_{j=1}^{n} x_{ij}=P_i, \quad i=1, \ldots ,m$$

$$\sum_{i=1}^{m} x_{ij}=Q_j, \quad j=1, \ldots ,n$$

where P_i $i=1, \ldots ,m$ are elements of vector P containing the row sum of X, and Q_j $j=1,...,n$ are elements of vector Q containing the column sum of X. It is also clear from the essence of the matrix that

$$\sum_{i=1}^{m} P_i=\sum_{j=1}^{n} Q_j$$

This implies that the estimation of m x n variables $x_{ij} \in \{0,1\}$ needs to be determined from m + n − 1 independent equations. Therefore, our problem is obviously underdetermined. Some previous research results (2,5,7) also show that the reconstruction of an arbitrary binary matrix from two projections is in general impossible. According to the theory by Ryser (1,2), it is possible to find zero, one, or more than one binary matrices satisfying a given pair of row and column sums (see Fig.2−1). To reconstruct the binary matrix, some certain assumptions always need to be made. In the following, we are going to review some of the research works done in this area and their assumptions.

	1	3	1	1	3	1
2	1	1	0	0	1	1
2	0	1	1	1	1	0
1	0	1	0	0	1	0

Two Solutions

	1	3	2	1	3	3
3	1	1	1	3		
2	0	1	1	3		
1	0	1	0	1		

One solution

No solution

Figure 2-1:

The matrix reconstruction algorithms can roughly be divided into two categories. The algorithms in the first category apply some direct methods to solve the matrices under some assumptions, while those in the other category usually reconstruct the matrix by using a priori knowledge, in other words, some predefined binary mask models. We will discuss some methods in both categories as follows.

The commonly used method in biplane angiocardiograms utilizes the assumption that the shape of the cross section is close to an ellipse (3). So the distance between two end points of each projection profile is taken as an axis of the ellipse. However, the shape of the cross section is usually not an ellipse, and the reconstruction result of a certain cross section also depends on the orientation of the cross section. In 1983, Eiho et al. (4) proposed a method to solve the orientation dependence problem by using three projection profiles with the same ellipse assumption. The reconstructed shape is much improved with the expense of one more projection, but still far from a shape of a real ventricular cross section. Chang (5) has developed an algorithm to recover any binary matrix from two projection profiles. The algorithm can obtain the exact reconstruction when there exists only one unambiguous solution from two projection profiles. However, most of the shapes of cross sections are ambiguous based on his definition. Only one in a large amount of possible solutions found by his algorithm is the real solution. So the results are usually not correct. Chang and Chow proposed another algorithm to specifically reconstruct the shape of a ventricle (6). They assumed the cross section of the ventricle should be in a connected region which is convex symmetric. So the ambiguity is largely reduced, only a few possible solutions remain after reconstruction. However, a cross section of the left ventricle is in general not convex symmetric (7,9). Therefore, we proposed our new algorithm without the convex symmetry assumption to fit more generally to the left ventricle.

Because the ambiguity was hardly solved by most of the direct methods, researchers also found another approach that uses a priori information. At first, Onnasch and Heintzen (7) and Onnash (8) developed an algorithm for binary reconstructiobn of the left or right ventricle from two projections that utilizes a

model database obtained from the cast study of ventricles. This method implies the estimation, for every matrix element, of its probability to belong to the ventricle. Recently, Slump and Gervranchs proposed a method also incorporated with a priori knowledge to reduce the ambiguity of the problem (9). A minimum cost capacitated network flow algorithm is adopted, which yields the optimal solution with respect to the selected binary matrix models. If the correct models are available, these model-based reconstruction methods usually give more promising results than the direct methods. However, a correct model is physically unavailable, in fact, it is the goal to be recovered by these algorithms. Our new algorithm reconstructs the binary matrix with the assumption that the equal-divisor curve of a cross section always exists. No binary matrix model is required, though the reconstruction results are pretty reliable. We will discuss it in the following sections.

CHAPTER 3

MATHEMATICAL CONSIDERATIONS

Suppose that V is a connected region in R^d ($d >= 2$) and $f(x) = 1_V(x)$, the indicator function of V. Define

$$p(x_1, \ldots, x_{d-1}) = \int f(x_1, x_2, \ldots, x_d)\, dx_d \tag{3.1}$$

and

$$q(x_2, \ldots, x_d) = \int f(x_1, x_2, \ldots, x_d)\, dx_1 \tag{3.2}$$

p and q are known as projections along x_1-axis and x_d-axis respectively. In practice, our observations are given as follows:

$$R_1(x_1, \ldots, x_{d-1}) = p(x_1, \ldots, x_{d-1}) + \varepsilon(x_1, \ldots, x_{d-1}) + \lambda_1 \tag{3.3}$$

$$R_2(x_2, \ldots, x_d) = q(x_2, \ldots, x_d) + \eta(x_2, \ldots, x_d) + \lambda_2 \tag{3.4}$$

where ε and η are known as noises centered at expectations and λ_1 , λ_2 are known as the expectations of noises. In continuous case, ε and η can be assumed to be stochastic processes and in descrete case, they are assumed to be two families of random variables. In practice, R_1 and R_2 can be computed from two photos which are taken along two orthogonal directions. The problem we are faced is how to reconstruct the shape of the subject V by using these two profiles, R_1 and R_2. The mathematical work concerning this problem includes

(i) estimation of the projections $\hat{p}$ and $\hat{q}$.

(ii) reconstruction of V, $\hat{V}$, by using $\hat{p}$ and $\hat{q}$.

Obviously, the first task is statistical and the second is geometrical. In this section, we shall discuss how to solve these two problems.

At first, we shall consider the noise free case. In this case, there is no need to estimate the projections and it is assumed that p and q are known, λ_1 and λ_2 are zeros. In our reconstruction approach, the two projection profiles are not equally treated. According to their usage, let us name p as the constructor (constructive profile) and q as the ruler (control profile), respectively.

In the sequel, we always assume that V are regular, namely, each straight line along x_1-axis or x_d-axis intersects V in a closed interval on the line, if they are not disjoint. Define the equal-divisor surface (ED) as follows:

$$D = \{(x_1, \ldots, x_{d-1}), \text{ there is an } X_d \text{ such that } (x_1, \ldots, x_d) \in V\}$$

For $(x_1, \ldots, x_{d-1}) \in D$, denote the two intersection points of the line $(X_1=x_1, \ldots, X_{d-1}=x_{d-1})$ and the surface of V by $(x_1, x_2, \ldots, x_d^0)$ and $(x_1, x_2, \ldots, x_d^1)$, i.e.,

$$x_d^0 = \sup \{x_d \ , \ (x_1, x_2, \ldots, x_d) \in V\}$$

and

$$x_d^1 = \inf \{x_d \ , \ (x_1, x_2, \ldots, x_d) \in V\}$$

Then the surface $\{(x_1, \ldots, x_{d-1}, (x_d^0 + x_d^1)/2), (x_1, \ldots, x_{d-1}) \in D\}$ is called the ED of V (or more definitely the ED of V along x_d-axis). For convenience, we also call the function $g(x_1, \ldots, x_{d-1}) = 1/2(x_d^0 + x_d^1)$ the ED of V.

The following propositions are evident.

Proposition 1. If the ED and the constructor of V are known, then V can be reconstructed uniquely.

Proposition 2. If the constructor is given, then V and its ruler are continuous with respect to ED in the following metrics:

$$d(V,V') = \int |l_V - l_{V'}| dx \tag{3.5}$$

$$d(q,q') = \int |q(x_2, \ldots, x_d) - q'(x_2, \ldots, x_d)| dx_2, \ldots, dx_d \tag{3.6}$$

and

$$d(g,g') = \int |g(x_1, \ldots, x_{d-1}) - g'(x_1, \ldots, x_{d-1})| dx_1, \ldots, dx_{d-1} \tag{3.7}$$

where $g = 1/2(x_d^0 + x_d^1)$ and g' is similarly defined for another subject.

The most difficult thing in reconstruction is that there is no unique solution. We have the following example.

Example 1. Suppose V_1 and V_2 are two identical ellipses except the long axis of V_1 coincides with the line y=x and the long axis of V_2 coincides with y=−x. Both of their centers are at origin. Then V_1 and V_2 have the same constructors and rulers.

To make the solution unique, we have to make further assumptions which can be justified by practical knowledge. For instance, the doctor can say the heart of a patient is tilted towards left by his experience.

In the following we will consider the case d = 2. Suppose p(x) is a continuous and unimodal function defined on the interval D = [a,b] with $p(a) \geq 0$, $p(b) \geq 0$, and $p(x) > 0$, $x \in (a,b)$. Let f be a function defined on [a,b].

Define

$$V(f) = \{(x,y) : x \in D, f(x) - 1/2p(x) \leq y \leq f(x) + 1/2p(x)\}$$

and define

$$q^{(f)}(y) = \text{Max}\{x_1 - x_2; (x_1,y) \in V(f) \text{ and } (x_2,y)\, r(\varepsilon)\, V(f)\}, \tag{3.8}$$

if V(f) is regular and if there is at least one point x such that $(x,y) \in V(f)$, and $q^{(f)}(y) = 0$ otherwise.

Suppose F is a class of functions defined on [a,b] satisfying:

(i) each f in F is nondecreasing and continuous,

(ii) for each f εF, V(f) is regular,

(iii) for any pair f_1, f_2 ε F, the set $\{x \varepsilon (a,b), f_1(x) \neq f_2(x)\}$ consists of at most two pieces of open intervals.

$$v = \{ V(f) : f \varepsilon F\} \tag{3.9}$$

and

$$R = \{q^{(f)} : f \varepsilon F\} \tag{3.10}$$

We have the following basic theorem.

Theorem 3.1 Under the assumptions given above, we have

$$F \leftrightarrow V \leftrightarrow R \tag{3.11}$$

Where $\leftrightarrow$ denotes one-to-one correspondence. The proof of Theorem 3.1 is given in a companian paper by some of the present authors.

Theorem 3.2 (Basic Reconstruction Theorem). Suppose V is a subject to be reconstructed, and suppose the constructor of V is P(x). Let F be a function class satisfying the conditions given in (3.9). Suppose the ED of V belongs to F (of course, this implies V is regular). Then V is uniquely determined by its ruler among V with respect to F.

Example: Suppose V is convex region in R^2 with ED being a straight line up-sloped P(x), x ε [0,a] and q(y), y ε [0,b] are its constructor and ruler respectively. Take

$$F = \{\alpha x + \beta,\ 0 < \alpha < b/a,\ 0 < \beta < b\}$$

Use P and F, we get the set V, then by Theorem 3.2 V is the only element in V

which has q(y) as its ruler. This example explains why our procedure given in section 4-1 works. Now let us extend the result from d = 2 to the general case. Let V be a convex region in R^d, d > 2. As earlier defined, let p and q be its two projections and let g be its ED. For any fixed $x_2 = x_2^0, \ldots, x_{d-1} = x_{d-1}^0$, define

$$V^* = [(x_1, x_d) : (x_1, x_2^0, \ldots, x_{d-1}^0, x_d) \in V]$$

$$p^*(x_1) = p(x_1, x_2^0, \ldots, x_{d-1}^0)$$

$$q^*(x_d) = q(x_2^0, \ldots, x_{d-1}^0, x_d)$$

and

$$g^*(x_1) = g(x_1, x_2^0, \ldots, x_{d-1}^0)$$

provided that V^* is not empty. Then V^* can be regarded as the cross section of V, cut out by the hyper plane $\{x_2 = x_2^0, \ldots, x_{d-1} = x_{d-1}^0\}$. Also, p^*, q^* and g^* are the constructor, ruler and ED of V^* respectively. It is easy to see that for each $x_2 = x_2^0, \ldots, x_{d-1} = x_{d-1}^0$, g^* is continuous and nondecreasing if and only if g is continuous and nondecreasing in x_1 for each fixed $x_2, \ldots, x_{d-1}$. Hence by theorem 3.2 we have

Theorem 3.3 Suppose that V is a regular subject in R^d to be reconstructed with nondamaged profiles $P(x_1, \ldots, x_{d-1})$ and $q(x_2, \ldots, x_d)$. Let F be a family of functions satisfying the conditions (3.9) for each given multiple $(x_2, \ldots, x_{d-1})$. Then the true subject V is the only one which has q as its ruler, among the family of subjects constructed by p and each element in F.

Here the regularity of region in R^d is similarly defined as that in R^2. Namely, a region V in R^d is called regular, if each line $\{x_1 = x_1^0, \ldots, x_{d-1} = x_{d-1}^0\}$ or $\{x_2 = x_2^0, \ldots, x_d = x_d^0\}$ can only intersect V in a closed interval (or a single point or empty).

Remark 1. Since the regions under usual consideration are assumed to be convex, thus the condition of regularity is satisfied.

By Theorems 3.2 and 3.3, the task of reconstruction turns out to estimate the ED of the region by using its two projections. Thus our problem becomes to fine a function among a given class of functions such that the derived projection along x_1−axis is closest to the observed one, the ruler.

By Weierstrassian approximation theorem, for any continuous function, we can find a polynomial uniformly approximating it. Thus we can restrict our attention to finding a polynomial as the estimate of the ED of V. The detail description of the reconstruction algorithm will be given in the following section.

Next, let us consider the case where noise arises. Because the projections p and q are damaged by the noise, we can not use R_1 and R_2 to do reconstruction and we have to smooth them to eliminate the affect of noise. There are many ways to do so. We only state several simple methods here.

(i) Kernel smoothing. Suppose K is a probability density. Choose a positive number h, then let

$$\hat{p}(x)+\hat{\lambda}_1 = \frac{1}{h^{d-1}} \int_{R^{d-1}} R_1(y)\, K\left(\frac{x-y}{h}\right) dy$$

$$\hat{q}(x)+\hat{\lambda}_2 = \frac{1}{h^{d-1}} \int_{R^{d-1}} R_2(y')\, K\left(\frac{x'-y'}{h}\right) dy'$$

(ii) Histogram smoothing. Split D into small regions as $D_1, D_2, \ldots, D_m$. Then define

$$\hat{p}(x)+\hat{\lambda}_1 = \frac{1}{|D_i|} \int_{D_i} R_1(y')\, dy, \text{ if } x \in D_i$$

Similarly smooth q as $\hat{q}$.

(iii) Median smoothing. Choose $\delta > 0$, for each x, take the median of the observations of p observed in the interval $(x-\delta, x+\delta)$ as the estimate $\hat{p}$ of R_1. Similarly define $\hat{q}$. This approach is available only for discrete case.

(iv) Polynomial fitting. Find a polynomial $\hat{p}$ which minimizes

$$\int [R_1(x) - (\hat{p}(x) 1_{[\hat{a},\hat{b}]}(x) + \hat{\lambda})]^2 dx$$

Similarly define $\hat{q}$.

Under certain conditions, we can prove all the above approaches get consistent estimates of the true profiles. The proof will be found on the other technical report which will be filled later soon.

CHAPTER 4

SHAPE RECONSTRUCTION

For a given cross section as in Fig. 2, one can have the two profiles from the column and row projections, where

$$\sum_{i=1}^{m} x_{ij} = P_j, \quad j = 1, \ldots, n ;$$

$$\sum_{j=1}^{m} x_{ij} = Q_i, \quad i = 1, \ldots, m ;$$

(4.1)

P_j and Q_i denote the two projection profiles and x_{ij}'s ε {0,1} are the cells in the given matrix. We assume that a cross section of a left ventricle is a connected region without holes in the m x n binary matrix X. Therefore, we can get the mass center of the cross section which can always be unambiguously determined from any given sets of profiles.

$$i_c = \bar{i} = \frac{\sum_{i=1}^{m} i \cdot Q_i}{\sum_{i=1}^{m} Q_i} \quad \text{and} \quad j_c = \bar{j} = \frac{\sum_{j=1}^{n} j \cdot P_j}{\sum_{j=1}^{n} P_j}$$

(4.2)

In general, we can find an ED curve, along which one of the projection profiles can be divided into two equivalent halves. For instance, in Figure 4-1, we can see the real ED curve divides P_j into two halves at $j = j'$, where one half is above the ED curve and the other half beneath it. Consequently, if we repeat this operation for $j = 0, \ldots, n$, along the real ED curve, the cross section can be correctly reconstructed from P_j. In other words, the proposition, that a cross section can

always be uniquely determined by one of its projection profiles and its corresponding ED curve, is always valid for any regular cross sections. Therefore, our problem is simply to estimate the real ED curve with respect to P_j or, similarly the real ED curve with respect to Q_i, which can divide Q_i, $i = 1, \ldots, m$ into two equivalent halves rowwise. Let us use the following equation to approximate the ED curve in Figure 4-1.

$$\hat{i}\ (j') = i_c + a_0 + a_1 (j' - j_c) + a_2 (j' - j_c)^2 + a_3 (j' - j_c)^3 \tag{4.3}$$

where (i_c, j_c) are the coordinates of the weight center, j' is the given j coordinate, and a_i, $i = 0, \ldots, 3$ is the parameter of vector A, with which we aproximate the real ED curve. Then we can assign

$$\tilde{x}_{ij} = \begin{cases} 1 & \text{if } |\hat{i} - i_c| \leq \tfrac{1}{2} P_j \\ 0 & \text{otherwise,} \end{cases} \tag{4.4}$$

If the approximation of ED curve in (3) is perfect, we can have

$$\tilde{Q}_i = \sum_{j=1}^{n} \tilde{x}_{ij}, \quad i = 1, \ldots, m$$

and

$$E_Q = \sum_{i=1}^{m} |Q_i - \tilde{Q}_i|, \tag{4.5}$$

where E_Q equals to zero.

From the same approach for $\tilde{P}_j$, we can also have

$$E_P = \sum_{j=1}^{n} |P_j - \tilde{P}_j| \tag{4.6}$$

,and E_P equals to zero if the estimation of ED curve is correct. The regularity

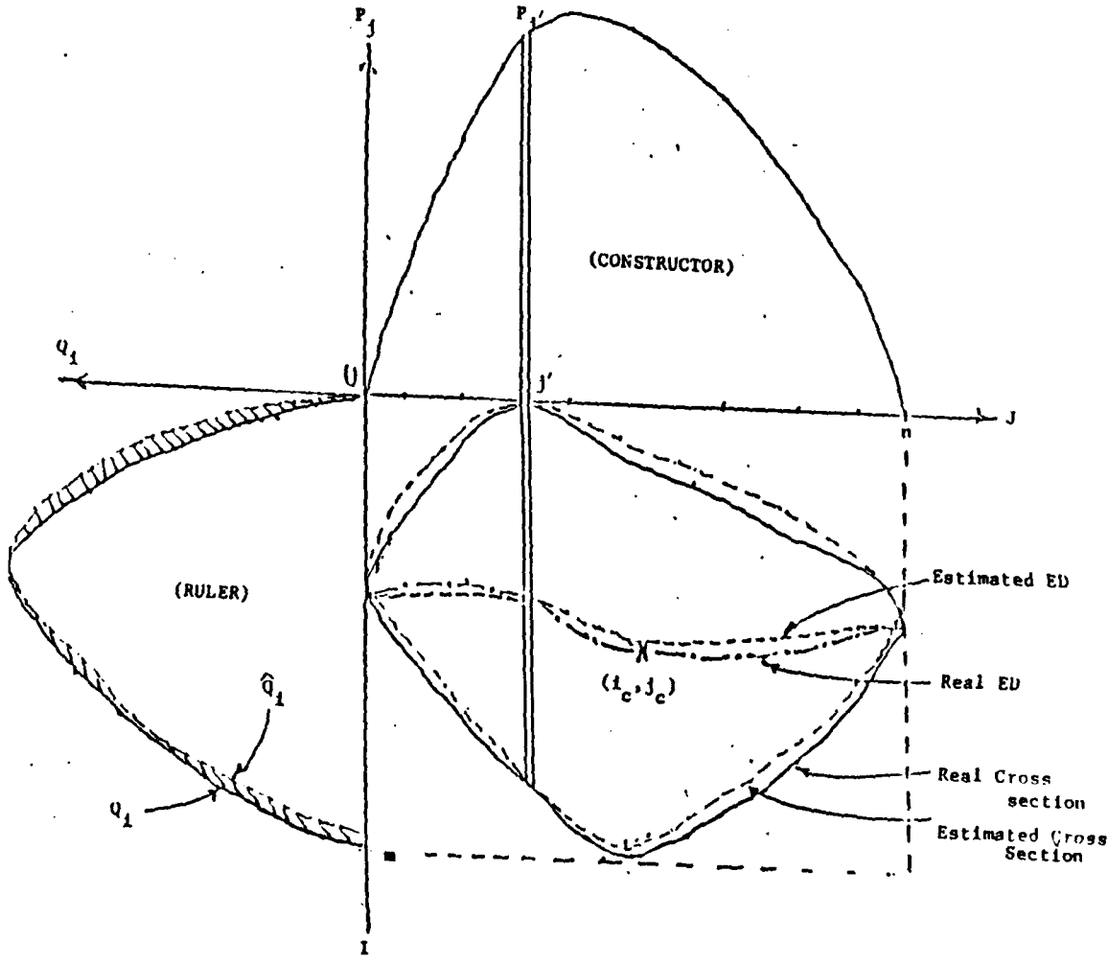
P_j
P_j'
(CONSTRUCTOR)
q_i
0
j'
J
n
(RULER)
Estimated ED
Real ED
(i_c, j_c)
Q̂_i
q_i
Real Cross section
Estimated Cross Section
I

Figure 4-1:

constraint in our algorithm is much less restrictive than the convexity constraint, since even the concave cross section can also be regular. Therefore, the regularity constraint fits the ventricular shapes much better. From a normal shape of ventricle, which does not have abrupt changes on its boundary to cause large discontinuities on ED curves, we usually can expect E_P and/or E_Q close to zero. So the cross section can be reconstructed if A can be obtained. Now we state that our problem is to find a optimal vector A which will minimize E_P or E_Q.

In the sequel, let us summarize our algorithm of reconstruction in several steps as follows. The detail of each step will be illustrated in the subsequent subsections.

Algorithm:

1. Find the weight center (i_c, j_c) of two projection profiles by using equation (4.2)

2. Assume ED is linear and passing through (i_c, j_c), *i.e.*,

   $$ED: \hat{i} - i_c = a_1 \cdot (j - j_c)$$

   or

   $$\hat{j} - j_c = a_1 \cdot (i - i_c).$$

   By using the coarse-to-fine approach, obtain a_1^*'s, which minimize E_Q or E_P.

3. Perform the consistency test to obtain the unique solution of a_1^* on each layer of cross sections.

4. Let ED be a curve approximated by a third order polynomial, such that

   $$ED: \hat{i} - i_c = (a_0 \pm \Delta a_0) + (a_1 \pm \Delta a_1)(j - j_c) + (a_2 \pm \Delta a_2)(j - j_c)^2 + (a_3 \pm \Delta a_3)(j - j_c)^3$$

   (Similarly for j coordinates)

   to minimize E_Q with respect to $A = [a_0, a_1, a_2, a_3]'$ by a gradual descent method with a fixed step ΔA. The a_1^* obtained in the last step is used as the initial value of a_1.

5. A contour relaxation procedure is then applied to obtain the higher order terms of the polynomial used to estimate ED curve. Therefore, it further refines the reconstruction results.

6. Regenerate each cross section. Pile them up slice by slice to construct the 3-D shape.

4.1. A COARSE-TO-FINE APPROACH TO FIND A_1^*

For a convex or slightly concave cross section, ED curve can roughly be approximated by a line. The direction of the estimated ED line implies the major orientation of the cross section. To obtain it, let us assume

$$i(j') = j_c + a_1(j'-j_c) \quad \text{at } j=j'$$
$$\text{(or similarly } j(i') = j_c + a_1(i'-i_c), \text{ at } i=i')$$

(4.7)

and find an optimal a_1^* such that from the reconstructed $\hat{x} \in \{0,1\}$, we can obtain E_Q^* or E_Q^*, where

$$E_Q^* = \underset{a_1}{\text{Min}}\, E_Q = \underset{a_1}{\text{Min}} \sum_i |Q_i - \hat{Q}_i|$$
$$\text{or } E_P^* = \underset{a_1}{\text{Min}}\, E_Q = \underset{a_1}{\text{Min}} \sum_j |P_j - \hat{P}_j|.$$

The procedure to find E_Q (E_P) has been described in the previous subsection by equations (4.4),(4.5),(4.6).

Since the minimum of E_Q(or E_P) can not be obtained analytically, we use a coarse-to-fine approach in finding a_1^*. As illustrated in Figure 4-2, we start with an array of five equally spaced a_1 values covering the possible range of a_1 $[-\alpha,\alpha]$. The three neighboring a_1's which contribute the least sum of three neighboring E_Q's (or E_P's) are picked up after each iteration. By inserting two new a_1's into the two slots between three picked a_1's, another array of five equally spaced a_1's is formed again. The array is then used to initiate another iteration. Ultimately, the optimal a_1^* is picked up from one of the five remaining a_1's which generate the smallest values of E_Q (or E_P) after four iterations of this procedure. Nevertheless, the a_1^* is not always unique. Two possible a_1^*'s can be generated if the project profiles of the ruler is symmetric with respect to its weight center The ED lines of the reconstructed cross sections are symmetrical with respect to the axis passing through the weight center and parallel to the constructor. In other words, these two a_1^*'s are similar in

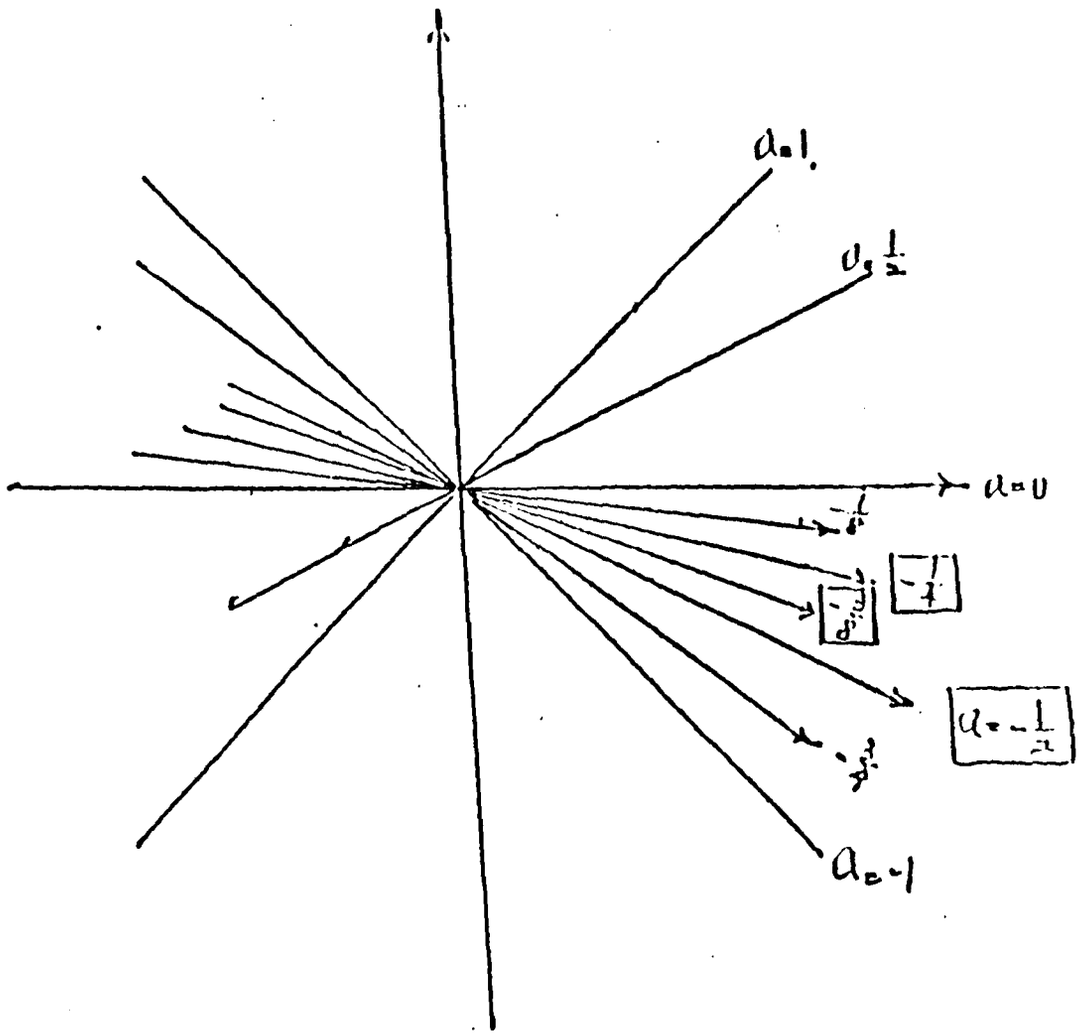

α = 1, □ is the selected center of group at each iteration.

Figure 4-2:

value but with different signs. Therefore, the other possible a_1^*'s, if available, can be found from the opposite portrait of the last five remaining a_1's. In this implementation both a_1^* and $a_1^{*'}$ are recorded for the next process, if the a_1^*s is not larger than a_1^* by 15%.

The reconstruction results from a vertical and horizontal constructor are usually different. Thus, the above process can be applied to both horizontal and vertical directions, but generate only one set of a_1^* from one of the directions. However, both sets of a_1^* are stored if both directions generate similar E_P and E_Q. This ambiguity may be caused by a cross section highly symmetric with respect to the origin. The consistency test procedure in the next subsection can be utilized to cope with this problem.

4.2. TEST OF CONSISTENCY

From a symmetrical ruler projection profile, two cross sections, which are symmetrical to each other with respect to the direction parallel to the direction of the constructor, can be reconstructed equally well. Therefore, the ambiguity arises when more than one cross section can be reconstructed from the same pair of projection profiles.

The first step of the reconstruction process under the assumption of a linear ED is performed exclusively with the two projection profiles given in the corresponding layer. In fact, it estimates the major orientation of the cross section on the current layer. Thus, the major orientation of the cross sections on all the layers can be obtained independently. The orientations and error indices of both possible answers on every ambiguous layer are stored. After computing cross sections on all the layers, the ambiguities can then be resolved by using the property that the cross

sections on neighboring layers are smoothly and continuously connected. Therefore their major orientations are consistent in similar directions.

To pick up the real orientation from the possible solutions of an ambiguous layer, the following two simple rules need to be applied.

Rule1: If both neighboring layers are unambiguous, then pick the one that gives minimum difference of orientations to both neighboring layers.

Rule2: If only one of the neighboring layers is unambiguous, then pick the one that gives minimum difference of orientation to the unambiguous cross section.

In general, the ambiguities generated by symmetric projection profiles on the ruler can be determined by inference from the neighboring layers.

The consistency of the major orientations affects the 3-D shape reconstruction substantially only when the reconstructed cross sections are elongated in shape. Due to the nature of the algorithm, the cross section reconstruction is more accurate when ED lies along the elongated direction. Therefore, the optimal ED lines obtained in step one usually are from the same side of constructors. One from the two possible solutions can be determined easily by using the two given rules. If the orientation of the cross section is tilted about ±45 degrees. the reconstructions by using horizontal or vertical projection profiles as constructors can both obtain fairly good results. It is preferred to use the same side of constructor as its two neighboring layers. However, the two neighboring layers may not use the same side of constructors in the transition area where the orientations of the cross sections change from less than to more than ±45 degrees. The two given rules are still applicable since the real ED lines of the horizontal and the vertical constructors are in similar orientations when their major direction of the cross section are around ±45 degrees. The orientation that generates minimum projection error(E_P or E_Q) and satisfies the two given rules is picked up in the transition case.

The process of the consistency test can be performed from top layer to bottom layer (and then in reverse if necessary) by using the results from the first step

It is comparatively less expensive in computation because point to point matching is unnecessary in our approach. Instead, the properties of ED line can be utilized. Thus , the consistent shape of 3-D objects is available, after this test, for the detailed adjustment in the following steps.

4.3. ITERATIVE DESCENT PROCEDURE TO ESTIMATE ED CURVE BY A POLYNOMIAL

The ED curve is not linear on some of the convex cross sections and most of the concave cross sections. The ED line obtained from the above process needs to be adjusted to better fit the real ED curve. Therefore, a third order polynomial is used to approximate the ED curve under the constraint that the weight center of the cross section is invariant. A higher order polynomial is intuitively easier to fit an arbitrary curve. In practice, a third order polynomial is usually moderate to simulate a nonlinear ED curve and computationally less expensive.

It is known that the weight center of the real cross section can be uniquely determined from the given two projection profiles. So, the weight center of the reconstructed cross section certainly should be always kept identical to the real one. As a result of this constraint, only three parameters need to be adjusted in the optimization process. Now, we begin to further refine the ED curve by using

$$\hat{i}(j') = i_c + (a_0^0 + \Delta a_0) + (a_1^0 \pm \Delta a_1)(j' - j_c) + (a_2^0 \pm \Delta a_2)(j' - j_c)^2 + (a_3^0 \pm \Delta a_3)(j' - j_c)^3 \tag{4.8}$$

(Similarly, for the other projection

$$\hat{j}(i') = j_c + (a_0^0 + \Delta a_0) + (a_1^0 \pm \Delta a_1)(i' - i_c) + (a_2^0 \pm \Delta a_2)(i' - i_c)^2 + (a_3^0 \pm \Delta a_3)(i' - i_c)^3$$

)

At first, let a_1^* be the initial value of a_1 and zero be the initial values of a_0- a_2, a_3 to form an initial vector of parameters, denoted by A_0. A fixed array of Δa_i, i= 1,2,3 are given such that the external boundary points are changed by at least one cell when the corresponding a_i varies with the amount Δa_i. The change of a_0 value simply moves the weight center of the reconstructed cross section away from the real weight center. So the a_0 value is only adjusted by the other parameters in order to compensate the generated deviations to the weight center when those parameters are changed. The iterative descent procedure is therefore applied only to three parameters of A_0; a_0 is kept updated when necessary. Four points denoted as $a_i^1 = a_i^0 \pm \Delta a_i$, where a_i^0 has not been adjusted in the previous iteration and $i \in \{1,2,3\}$, are checked to find the optimal a_i^* which results in a minimum $E_Q(E_P)$, called $E_Q^*(E_P^*)$. If $E_Q^*(E_P^*) < E_Q^0(E_P^0)$, then $a_i^0 = a_i^*$. This process is repeated till no further improvement can be made. The final vector of A° is then the optimal solution of the problem that generates minimum sum of error between the real and estimated projection profiles.

4.4. CONTOUR RELAXATION

The real ED curve of a cross section can fairly be approximated by a third order polynomial. However, the attempt to obtain the exact ED curve still involves some higher order terms. To resolve these higher order terms by increasing the order of the polynomial which is used to approximate ED curve is too computationally expensive. The contour relaxation algorithm is designed to solve this problem without directly computing the higher order polynomials. Based on the theory, it minimizes the difference between the given and estimated projection profiles in order to minimize the difference between given and estimated cross sections under the condition that the regularity constraint on the contour of the cross section

should not be violated. The difference between the real and estimated ED curves introduces error represented as the difference between the estimated and given projections along the ruler coordinate. It is clear from our proposition that the real cross section can be uniquely reconstructed from a given constructor and its corresponding real ED curve. Therefore, the contour relaxation algorithm intends to eliminate the difference between given and estimated projection profiles to obtain the estimated ED as correct as possible. Now let us introduce the algorithm in the following.

To simplify the illustration, we use a horizontal constructor as in Figure 4-3; the alternative case can be solved similarly. First, let us set the projection error e(j) as the projection of estimated cross section minus the real given projection at each row j along the ruler coordinate. The upward potential $U_i(k)$, and downward potential $D_i(k)$, which will be explicitly defined later, at each column i along the constructor coordinate are used as the basic measures in this algorithm. As we know, the deviation between real and estimated ED's generates the difference between estimated and ruler projection profiles, and contributes error to the projection error e(j). This error can obviously be compensated by shifting the estimated ED upward or downward toward the real ED. However, the real ED is unknown. Therefore, the adopted $U_i(k)$ and $D_i(k)$ represent the potential to reduce error by shifting upward or downward along column i from point k-1 to point k away from the current estimated ED. It is obvious that the potential of shifting upward or downward increases when large projection error can be compensated after the shifting. From Figure 4-3, we define $U_i(k)$ and $D_i(k)$ as below.

Let m_i and n_i denotes the row coordinates of the upper and lower boundaries of the estimated cross section at column i. Moving this column one point upward (k=1) will make the projection error $e(m_i+1)$ increase one while $e(n_i)$ will decrease one. Therefore, larger $e(n_i)$ and smaller $e(m_i+1)$ implies more potential to move this column upward. Thus, we define

$$U_i(1) = e(n_i) - e(m_i+1),$$

and

$$U_i(k) = e(n_i+k-1) - e(m_i+k),$$

when the column is moved from point k−1 to point k upward. Similarly, for shifting downward, we define

$$D_i(1) = e(m_i) - e(n_i-1),$$

and

$$D_i(k) = e(m_i-k+1) - e(n_i-k).$$

Using U_i and D_i, we then define

$$TU_i = 2 \cdot U_i(1) + U_i(2) + U_i(3)$$
$$TD_i = 2 \cdot D_i(1) + D_i(2) + D_i(3)$$

and

$$f(i) = TU_i, \quad d(i)=1, \quad \text{if } TU_i - TD_i > T_i$$
$$f(i) = TD_i, \quad d(i)=-1, \quad \text{if } TD_i - TU_i > T_i,$$
$$f(i) = 0, \quad d(i)=0, \quad \text{ortherwise,}$$

where $T_i = 0.75\ \text{Max}(\ TU_i\ ,\ TD_i\ )$.

To include the influence from the neighboring columns, we then assign

$$g(i) = d(i-1)\cdot f(i-1) + 2d(i)\cdot f(i) + d(i+1)\cdot f(i+1),$$

to be used in the iterative process.

The TU_i (or TD_i) from the linear combination of U_i (or D_i) assigns more weight to the columns need to be shifted more deeply upward(downward). The f(i) and d(i) are then defined so that each column i can only be shifted upward, downward, or kept still. The larger the f(i) implies the more potential to move this column. Considering neighboring columns are usually shifted smoothly in the same direction, g(i) grants priority to the column where both its neighbors and itself have a strong tendency to be adjusted. Now let us state the contour relaxation algorithm as follows:

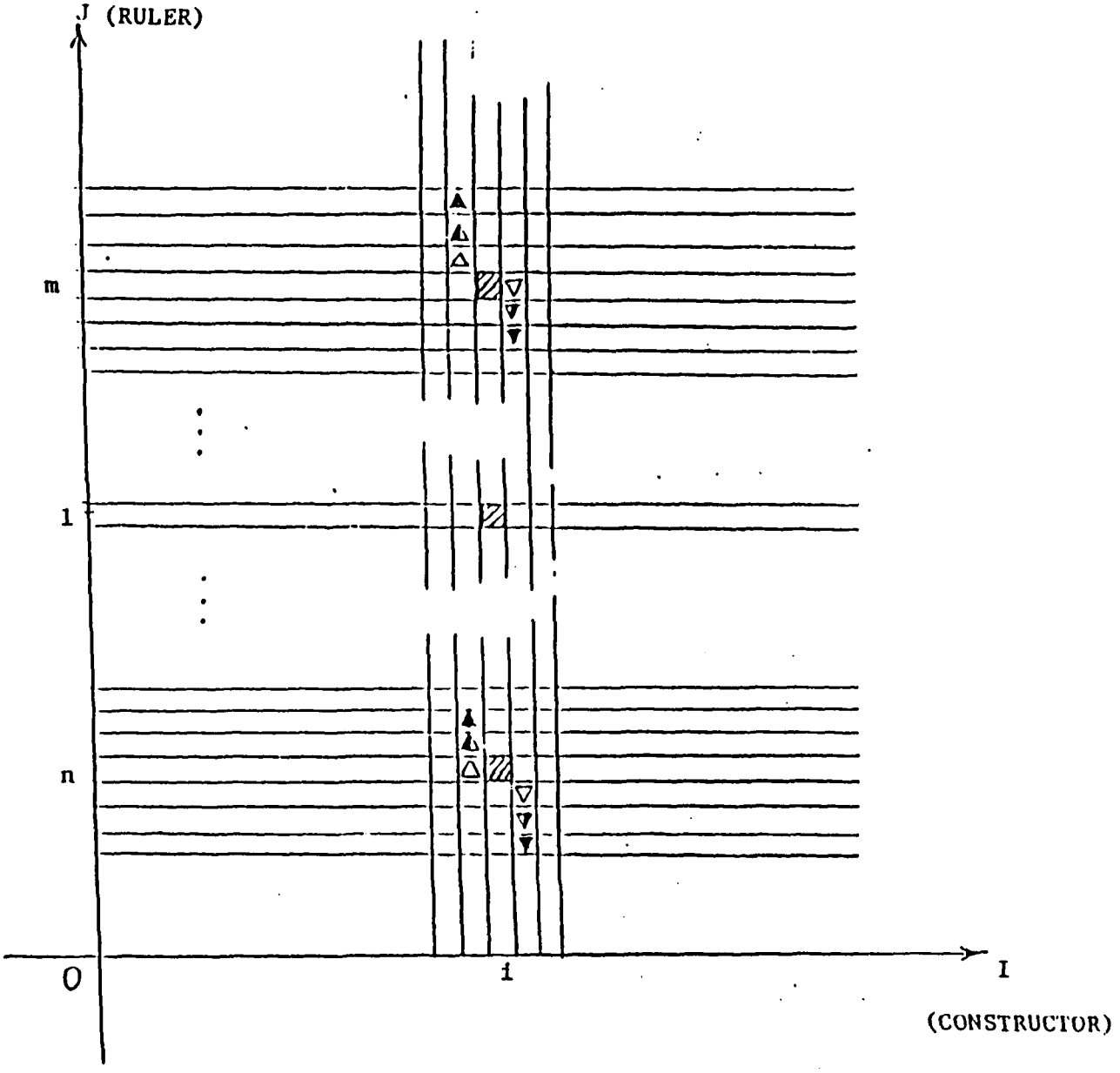

△ ◭ ▲ : Corresponding pairs for $U_i(k)$, k=1,2,3, respectively.

▽ ▼ ▼ : Corresponding pairs for $D_i(k)$, k=1,2,3, respectively.

Figure 4-3:

1. Adjust those columns which exceed the upper and lower end points of the ruler to assure the contour is within the possible region of cross section.

2. Let k=0. Obtain the initial $e^k(j)$ for each row on the ruler from the estimated cross section.

3. k=k+1. Compute $g^k(i)$ and $d^k(i)$ from $e^{k-1}(i)$ for each column i on the constructor.

4. For each row j with $e^{k-1}(j) \neq 0$, pick up a column with maximum $g^k(i)$ among those candidates, which reduce $|e^{k-1}(j)|$ by shifting according to $d^k(i)$, without violating the regularity constraint of the boundary.

5. For each picked column i, adjust it by shifting toward the direction given by $d^k(j)$ and then set $d^k(j)=0$. If the $d^k(j)$ has been set to zero, do no adjustment. Compute $e^k(i)$ after all columns have been adjusted.

6. If $E= \sum_j |e^k(j)|$ is reduced, go to 2, else stop.

Figure 4-4 demonstrates an example for the use of the contour relaxation algorithm. Figure 4-4(a) is obtained from the ED curve approximated by a third order polynomial. Figure 4-4(b) shows the results after applying this algorithm. Considerable improvement has been made by the contour relaxation. In fact, the algorithm can generally further refine the reconstructed cross section as long as the regularity is satisfied. The higher order terms of the estimated ED curve are resolved implicitly.

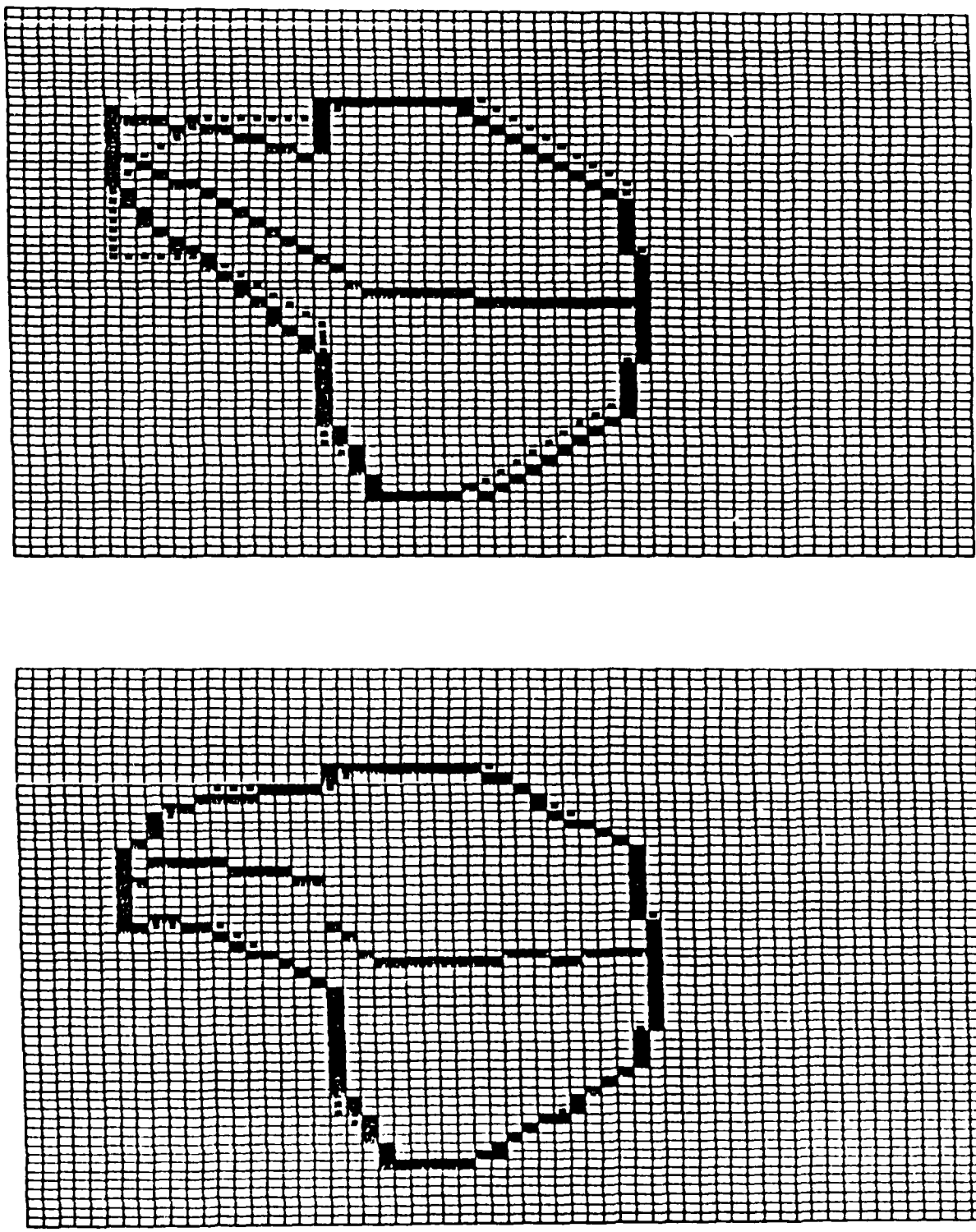

Figure 4-4:

4.5. SOME EXAMPLES OF THE CROSS SECTION RECONSTRUCTION

Some examples of the cross section reconstruction are given in this section Figures 4-5 to 4-10 illustrate some of the experimental results with our algorithm for six randomly drawn cross sections Each cross section is drawn by a graphic program into a 60 x 60 matrix. The projection profiles are constructed by summing up the elements belonging to the region of cross section columnwise or rowwise The reconstructed cross section is compared with the original. The relative mean error used in (6,11,12) is adopted to measure the performance. It is defined as

$$R = \frac{\sum_{i=1}^{m}\sum_{j=1}^{n} |Q_{ij}-x_{ij}|}{\sum_{i=1}^{m}\sum_{j=1}^{n} Q_{ij}} \qquad (4.9)$$

The Q_{ij} are the elements of the original cross section and x_{ij} are the elements of the reconstructed one. As mentioned above, the reconstruction does not refer to any predefined binary mask models However the results are quite good even when the original cross section is very irregular. Table 4-1 summarizes the experimental results for the cross sections shown in Figure 4-5 to 4-10. For each figures set, (a) shows the original cross section, (b) illustrates the reconstructed results and the estimated ED curve given by our method, (c) is the reconstruction results obtained by the ellipse approximation method. The dark curve inside the reconstructed region in (b) is the ED curve obtained by our algorithm. From 50 randomly drawn pictures, the reconstruction results for a regular shape ususlly can achieve more than 96% conformity, which is better than the results shown in (4.5). The conformity measure is given by the number of elements common to the original and the reconstructed cross sections Thus the conformity measure is one hundred minus half of the relative error R in percent. As to the cross sections of irregular shape, we usually get less than 20% R, in other words, it is around 90% conformity. Figure 4-5 to 4-10 show fairly regular cross sections: the results are as good as predicted

Figure 4-9 and 4-10 show cross section with obvious irregularity, which is generated by large concavity and sharp changes on boundary. Although the cross sections are irregular, the reconstructed results still keep the approximate shapes for visual recognition. In the next section, we are going to do the experiments with real X-ray pictures.

Table 4-1: Experimental results for Figures 4-5 to 4-10

Figure No.	Total No. of Points	Our Method			Ellipse Approximation		
		No. of Mismatch	R	Conformity	No. of Mismatch	R	Conformity
4-5	1733	128	7.4%	96.3%	778	44.9%	76.5%
4-6	1296	20	1.5%	99.2%	505	39.0%	80.5%
4-7	1382	44	3.2%	98.4%	840	61.7%	79.1%
4-8	970	24	2.5%	98.8%	298	30.6%	84.7%
4-9	1743	110	6.3%	96.8%	603	34.7%	82.6%
4-10	1322	150	11.3%	94.3%	624	47.2%	76.4%

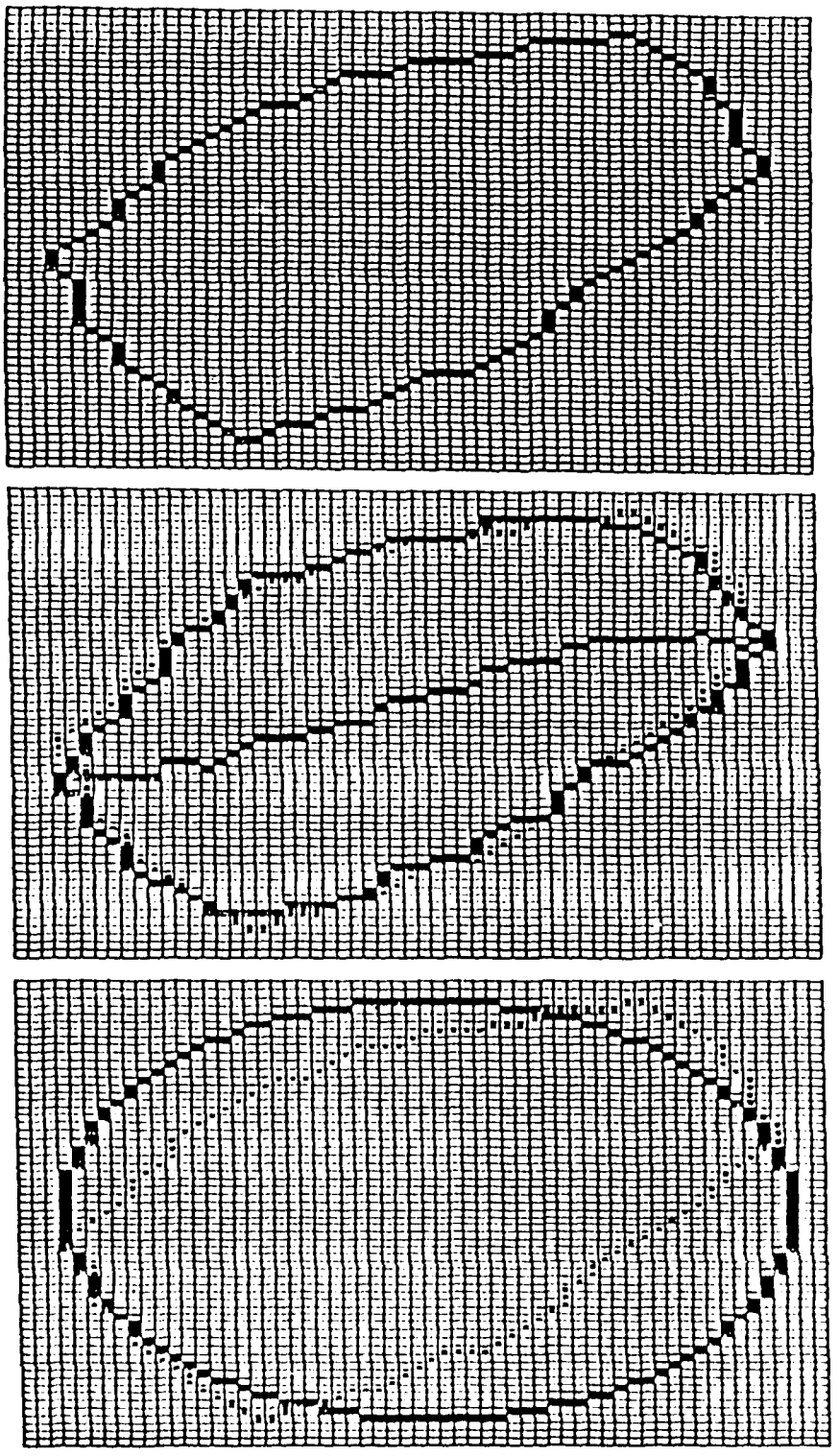

Figure 4-5:

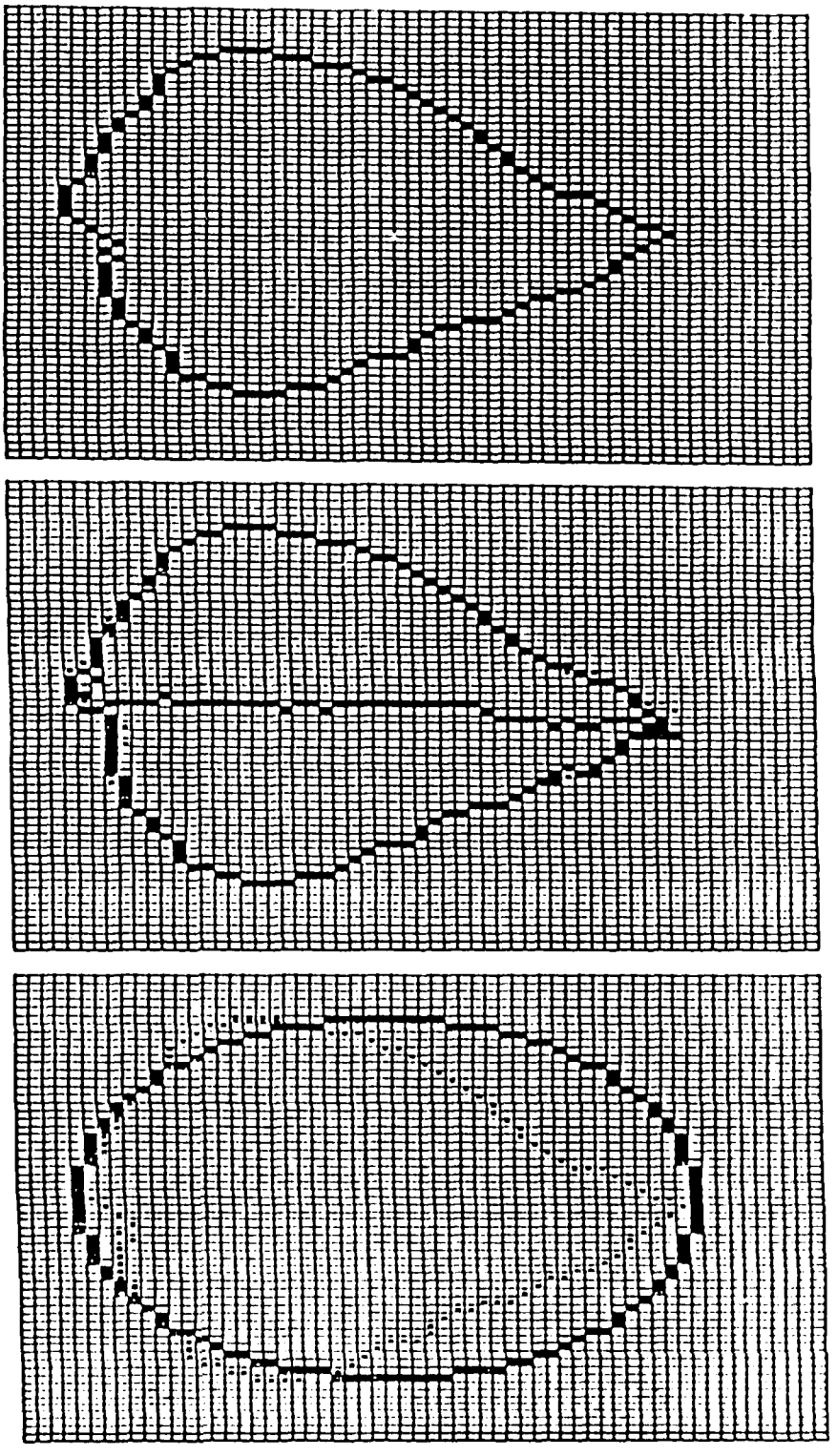

Figure 4-6:

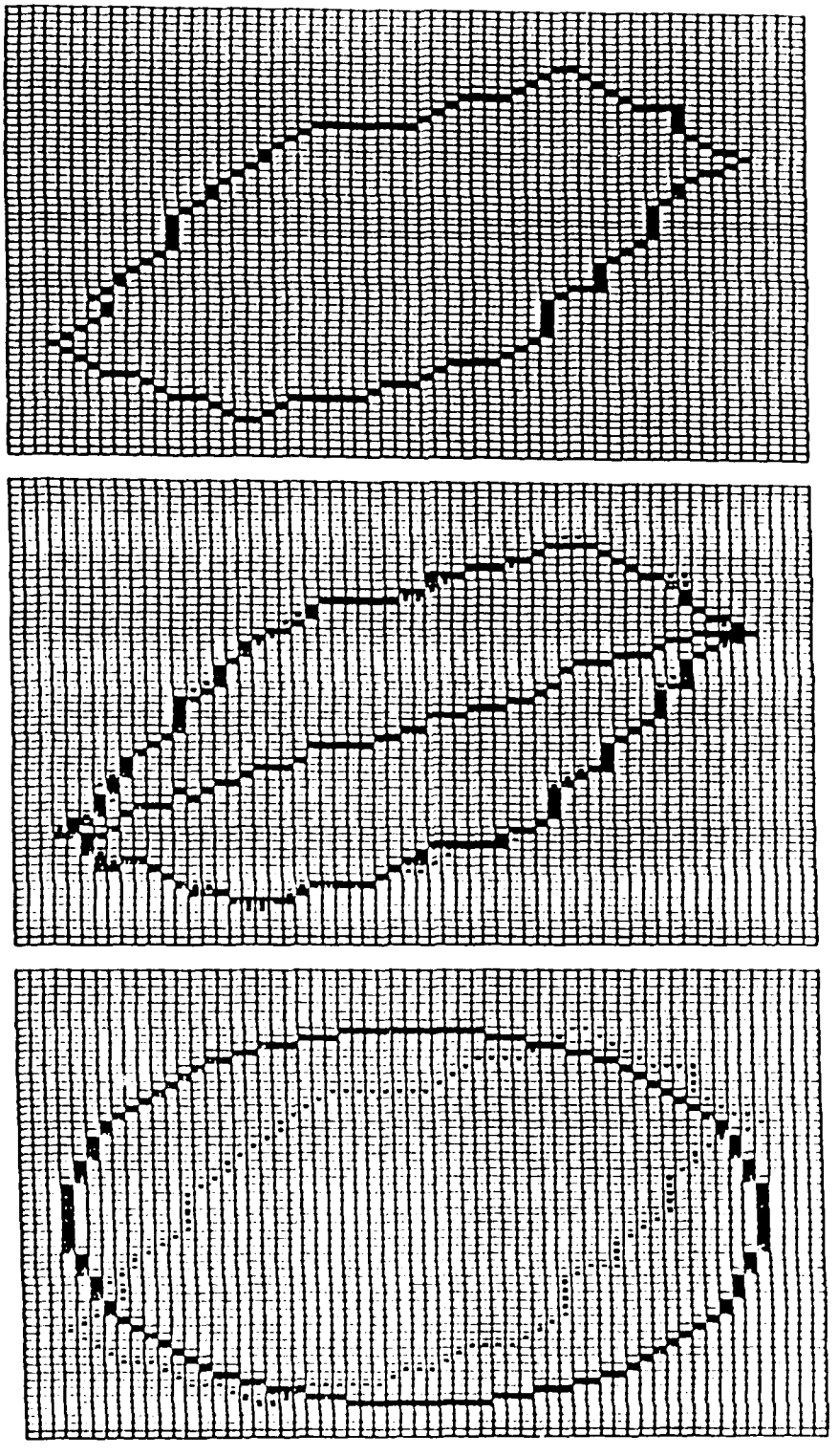

Figure 4-7:

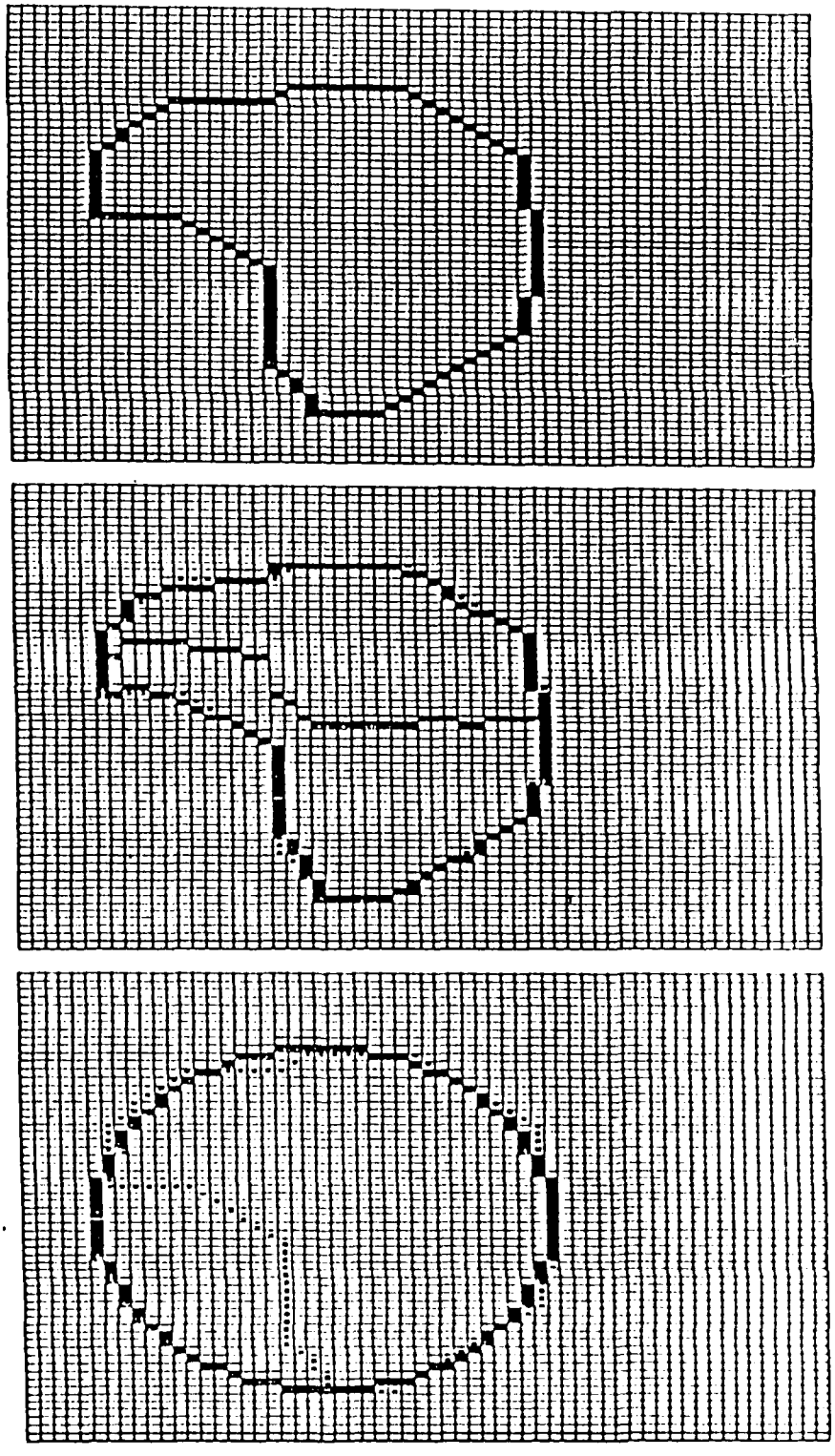

Figure 4-8:

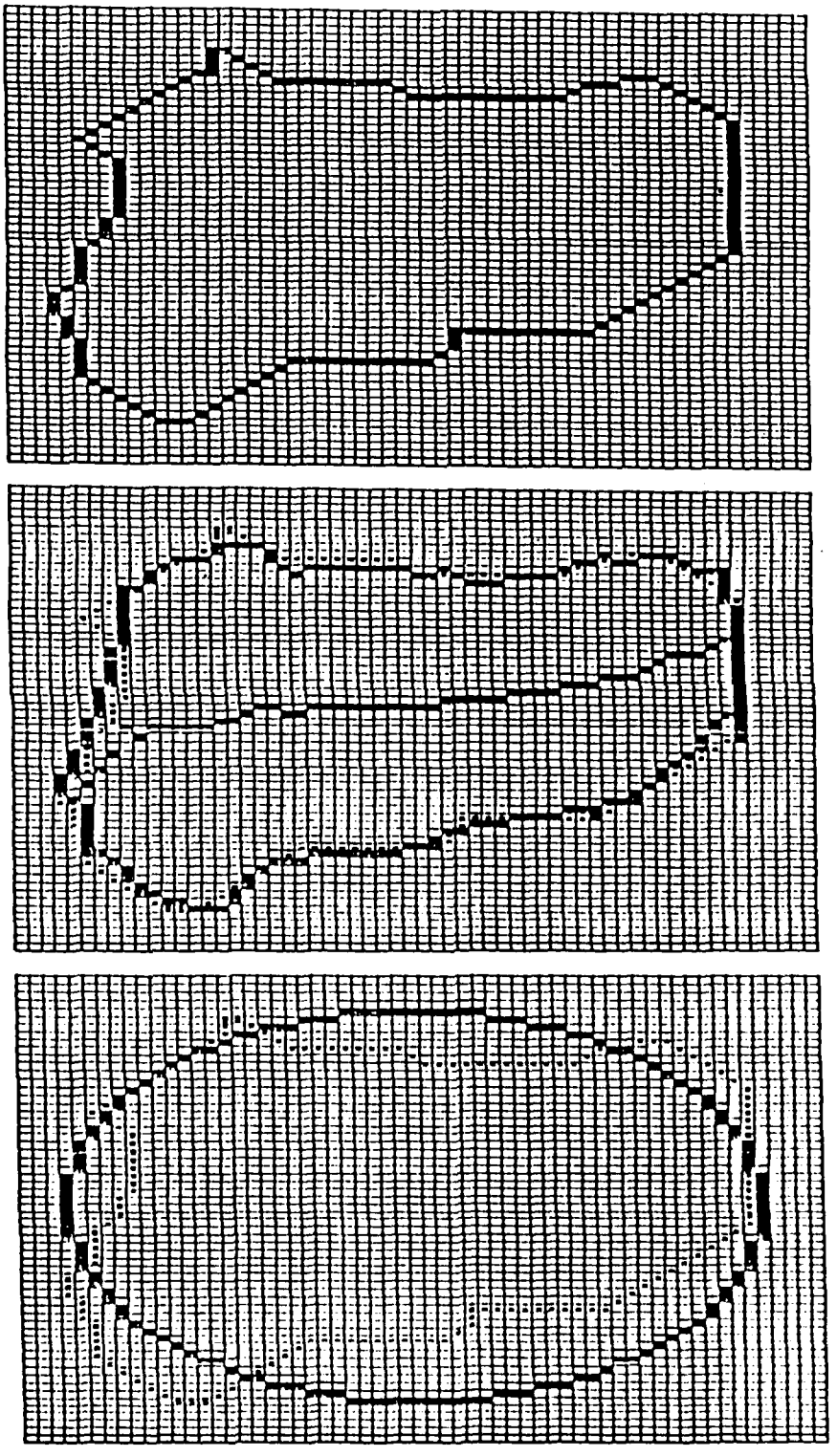

Figure 4-9:

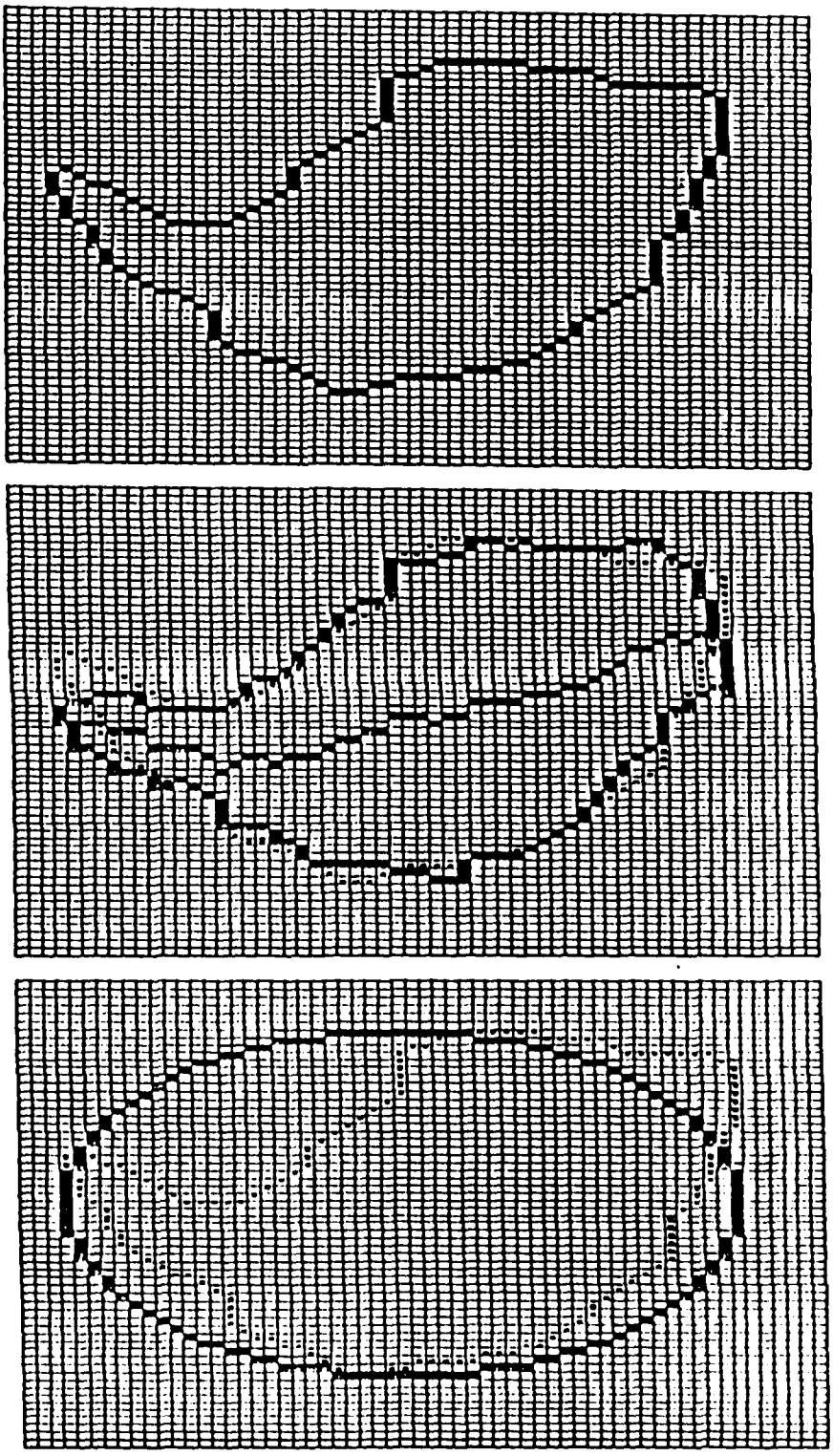

Figure 4-10:

CHAPTER 5

AN EXPERIMENTAL RESULT

In this section, we will demonstrate an example with two X-ray films of a bag of dye to show the applicability of the object reconstruction technique described in Section 3. The procedure of object reconstruction is shown in Figure 5-1. The films were digitized by an Optronix drum scanner into 512 by 512 arrays of pixels. The grey value of each pixel is recalled by an 8-bit integer which scales the intensity of brightness into the range between 0 and 255. Low grey value represents low intensity (dark pixels), while high grey value represents high intensity (bright pixels). The second step is to apply the logarithmic transformation to both left and right digitized images, such that the exponential absorption of the radiation is compensated. Then, the grey value of the dye free region is subtracted from the image since we are only interested in the net X-ray absorption by dye, which is proportional to the depth of the ventricle.

For a real ventricular reconstruction, we have to do some averaging work to assure the quality of image because the mixture of the injected dye is usually incomplete. However, this experiment utilizes a full bag of dye, so the incomplete mixture problem does not have to be considered in this case. The next step is the ventricular boundary detection. Several papers have been presented for this problem. Pope et al. utilize the Dynamic Search Algorithm (11) and Bocker utilizes the Laplacian-Gaussian operator (12), which are pretty reliable for the ventricular boundary detection . In this experiment, we utilize a simple threshold method to segment the region of object. The detected boundary is satisfactory since the used object is 150 cc of pure dye in a plastic bag whose shape is regular and unambiguous.

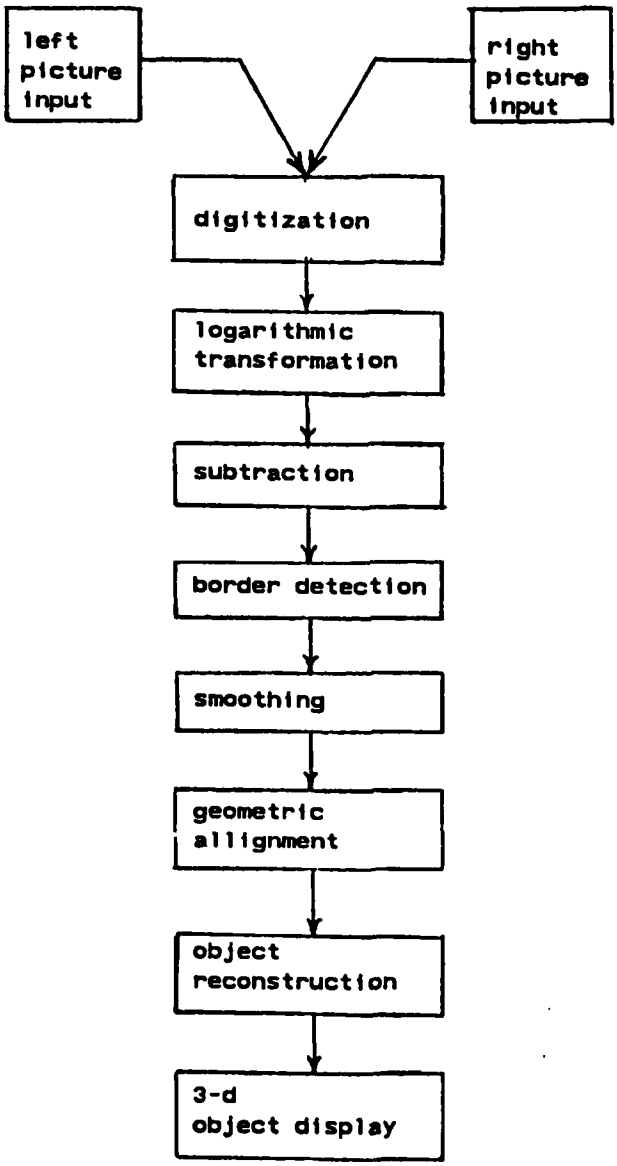
left
picture
input
right
picture
input
digitization
logarithmic
transformation
subtraction
border detection
smoothing
geometric
allignment
object
reconstruction
3-d
object display

Figure 5-1:

After the boundary detection, the segmented region is smoothed by a medium filter for eliminating the corrupted noise at the present experiment. The processed images are ready to use except their sizes are different since they were taken by two different sets of cameras. Therefore, these two images are scaled and aligned so that we can slice the two images into corresponding arrays of pixels. Each cross section will then be reconstructed from the grey values of the corresponding pair of pixel arrays. However, we can not apply these grey values directly into the binary reconstruction process because grey value is not equivalent to the depth of the object. Fortunately, the depth of the object and grey level are proportional to each other. It can be expressed by

$$D_x(i) = \alpha \cdot I_x(i)$$

where D_x is the depth, I_x is the grey value, and α is an adjustment coefficient decided by the characteristics of the X-ray machine. In this experiment, the α values for both projections are unknown. For simplicity, we assume the highest grey value corresponds to the width of the grey level profile on the other projection. So these two adjustment coefficients can be decided and used to transfer grey level profiles into depth profiles. The generated depth profiles are then used to reconstruct the cross sections. The reconstructed cross sections are put into a stack to represent the three-dimensional objects. On the other hand, the volume of the object is also computed with a Simpson integration formula,

$$\text{Volume} = h/3 \left(\sum_{\text{odd}} 4 \cdot \text{area} \right) + \left(\sum_{\text{even}} 2 \cdot \text{area} \right)$$

Figure 5-2 shows the original X-ray pictures for both left and right projections. Figure 5-3 shows the same image after preprocessing. Figure 5-4 shows the reconstructed three-dimensional object by piling up each reconstructed cross section. The estimated volume of this object is 153.2 cc, which is around 97.9% accurate with respect to the real volume 150 cc. The ellipse method by the H.P. ventricle estimation system obtains 163 cc for the object, which is around 91.4% accurate. Our method obtains better volume estimation, and the reconstructed shape (Fig. 5-4) is close to the real shape of the object according to doctor's observation.

Figure 5-2:

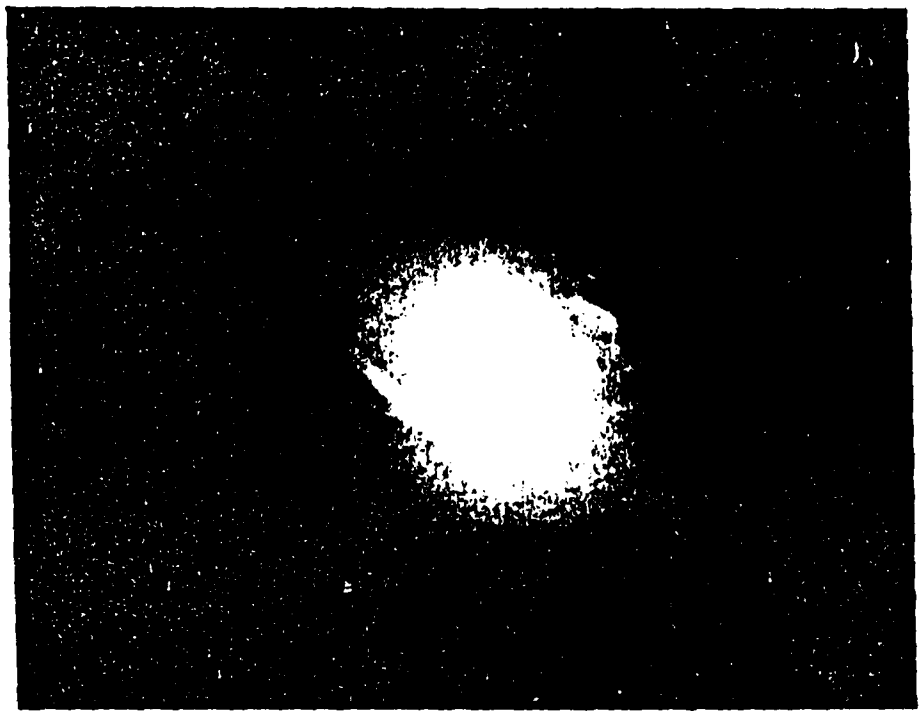

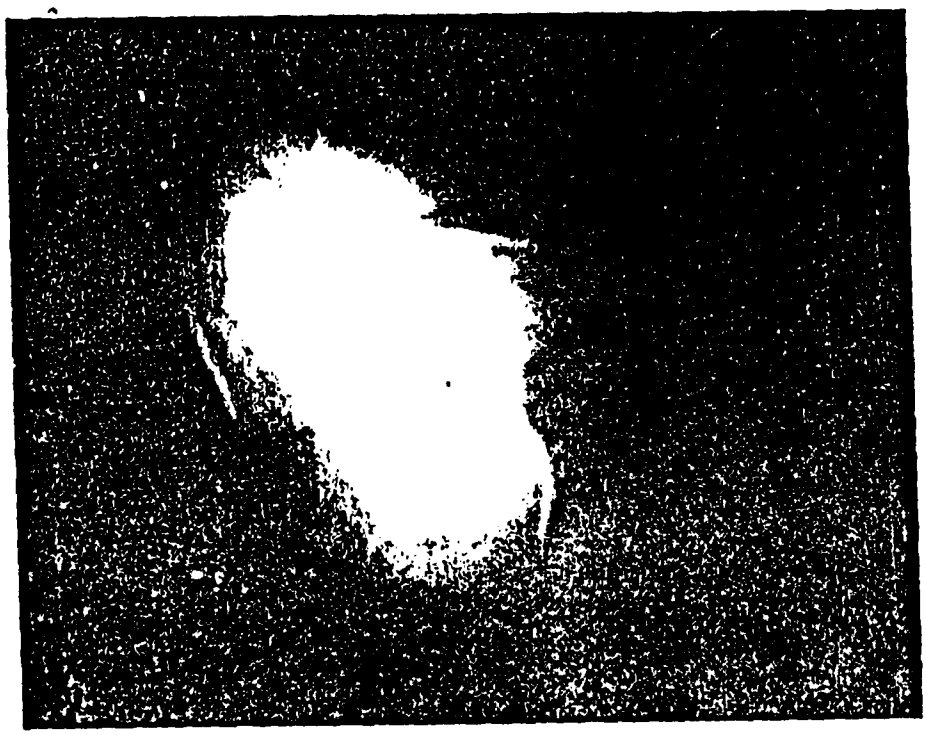

Figure 5-3:

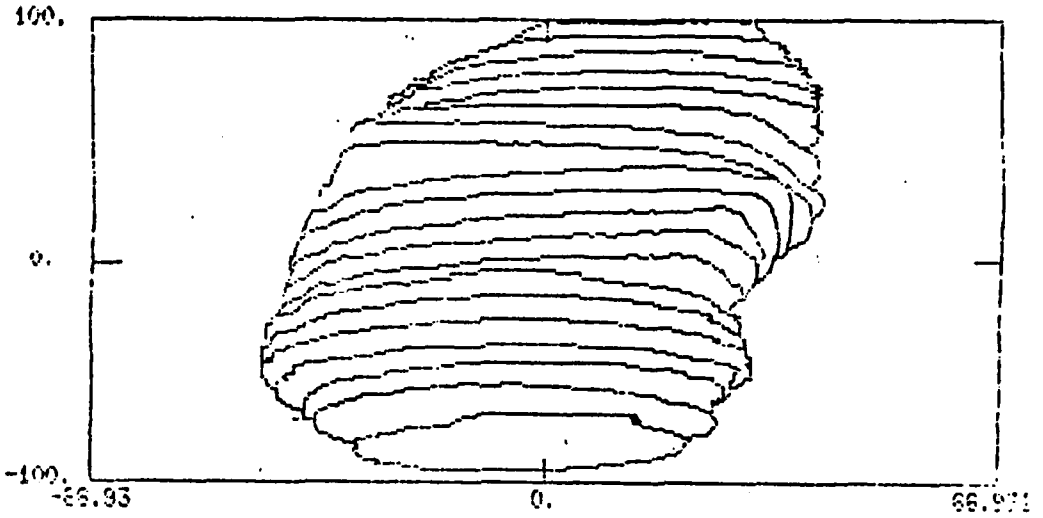

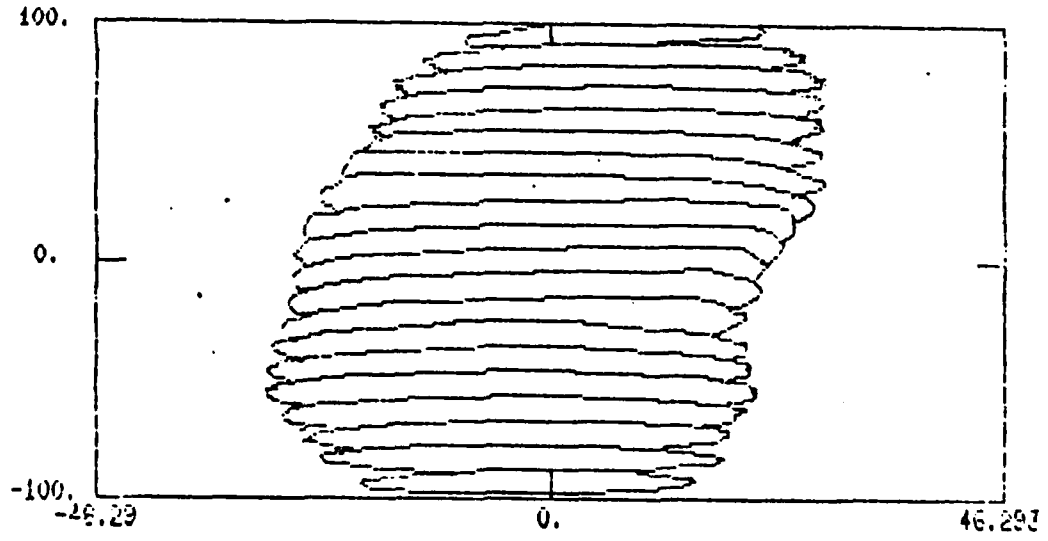

Figure 5-4:

CHAPTER 6

CONCLUSIONS AND SUGGESTIONS FOR FURTHER IMPROVEMENT

In this report, we present a new method to reconstruct the three-dimensional shape and estimate the volume of an object by using its two orthogonal projections. We have proved that the cross section can be optimally reconstructed by minimizing an error index which is generated by the sum of the absolute difference between the original and the estimated projection profiles. This error index is uniquely and continuously proportional to the sum of error between the original and the estimated cross sections under the condition that the original cross section is regular and has a monotonically non-decreasing or non-increasing equal-divisor curves. A new algorithm has been designed based on these properties.

The algorithm has been tested on synthetic cross section as well as real X-ray pictures. From synthetic pictures, it achieves better than 96% conformity for regular cross sections and better than 91% conformity for irregular ones. The reconstruction for X-ray pictures is also better than 95% conformity in every layer of cross section. The processing speed is less than 3 seconds for each cross section by a Fortran implementation in VAX 780. Thus, the algorithm are reliable and fast for the different experiments that we have done so far.

In the next phase of this project, we are going to apply this algorithm to real ventricular images. To obtain better results in real ventricular images, we suggest to further investigate the adjustment coefficient α of X-ray absorption. We also propose some methods to depress the corrupted noise in real X-ray images. At last, some more detail consideration will be made to directly reconstruct 3-D objects from the two projection images. Some more studies for the irregular case is also of interest.

REFERENCES

1. H.J. Ryser, "The Combinatorial Properties of matrices of zeros and ones", Canad.J.Math., 9, 1957, pp371-379.

2. H.J. Ryser, "Combinatorial Mathematics" Wiley, New York, 1963.

3. H.T. Dodge, et al, "The Use of Biplane Angiocardiography for the Measurement of Left Ventricular Volume in Man", American Heart Journal, 60(5), 1960, pp762-776.

4. S. Eiho, et al, "Reconstruction of the Left Ventricle from X-Ray Cineangiocardiograms with a Rotating Arm" Proc. 1983 IEEE Conf. Computer Cardiology, pp63-67.

5. S.K. Chang "The Reconstruction of Binary Patterns from Their Projections", Commu. of the ACM, Vol. 14, No. 1, Jan. 1971, pp21-25.

6. S.K. Chang & C.K. Chow "The reconstruction of binary patterns from two orthogonal projections and its application to cardiac cineangiography" IEEE Trans. Computer C-22 1973, pp18-28.

7. D.G.W. Onnasch and P.H. Heintzen "A new approach for the reconstruction of the right and left ventricular form from biplane angiocardiographic recordings." Proc. 1976 IEEE Conf. Computer Cardiology, pp67-73.

8. D.G.W. Onnasch "A concept for the approximate reconstruction of the form of the right or left ventricular from biplane angiograms" in Roentgen-Video-Techniques for Dynamic Studies of Structure and Function of the Heart and Circulation (P.H. Heintzen and J.H. Bursch, eds.), pp235-242. Thieme Verlag, Stuttgart 1978.

9. C.H. Slump and J.J. Gerbrands "A Network Flow Approach to Reconstruction of the Left Ventricle from Two Projections" Computer Graphics and Image Processing, 18, 1982, pp18-36.

10. Z.D. Bai et al, "Reconstruction of the Binary Matrix by the Theorems of the Equal-Divisor Curve" Internal Report, Center for Multivariate Analysis, Univ. of Pittsburgh.

11. D.L. Pope, et al, "Left Ventricular Border Recognition Using a Dynamic Search Algorithm", Radiation Physics, 1985, pp513-518.

12. E.R.P. Bocker, et al, "Experiments with 3D-Reconstruction From Ventriculograms Using Automatic Contour Detection" Technical Report 85/1 IMDM, Universitats-Krankenhaus Hamburg-Eppendorf(UKE).

END

5-81

DTIC